

Degree of paraxiality of a multi-Gaussian beam diffracted by a circular aperture

JINPING CHENG, YINGYING XIAO, HAO WU, XIAOLING JI, TAO WANG*

Department of Physics, Sichuan Normal University, Chengdu 610068, China

*Corresponding author: towerwang@126.com

The degree of paraxiality (DOP) of a diffracted multi-Gaussian beam is discussed. It is shown that the DOP of the multi-Gaussian beam will decrease as it is diffracted by a circular aperture, and the DOP of the diffracted multi-Gaussian beam is influenced by both the aperture radius and the characteristics of beam source. As an example, the dependence of the DOP on the aperture radius, the boundary characteristic, and the beam waist width is investigated.

Keywords: multi-Gaussian beam, diffraction, degree of paraxiality.

1. Introduction

With the continuous development of laser technology, the researches on the propagation and transformation of light beams have been extended from paraxial field to non-paraxial field [1-6]. The non-paraxial beam, namely a beam with a large divergence angle or a spot size that is equal to or even smaller than wavelength, can be produced by the solid-state laser, microcavity, or beams tightly focused with a high numerical aperture [7-11]. These beams are useful in optical data storage, optical trapping and high-resolution microscopy [12-15]. It is well known that non-paraxial and paraxial beams are studied using a variety of different theories and approaches. Therefore, determining whether a beam is paraxial or not is crucial to the thesis. Quantitatively describing the paraxiality of beams, which GAWHARY and SEVERINI introduced in 2008 by defining a physical quantity called degree of paraxiality (DOP), is an effective method for resolving this issue [16]. In 2010, GAWHARY and SEVERINI generalized the definition of DOP to make it describe the paraxiality of beams more accurately [17]. Subsequently, the DOP of different beams has been studied, including the Airy beam, the cylindrical vector partially coherent Laguerre–Gaussian beam, the stochastic electromagnetic Gaussian Schell-model beam, and others [18-23].

On the other hand, due to its special characteristic of flattened top distribution with adjustable edges, the multi-Gaussian beams have attracted much attention, especially its propagation characteristics through turbulence and various optical systems [24-26].

In practical optical systems, apertures often serve as the limit for laser beams. In this situation, the aperture will affect the optical characteristics of beams, including its DOP [27-30]. For example, the DOP of Gaussian beams diffracted by a circular aperture is smaller than that of non-diffracted Gaussian beams [31]. However, as far as we know, there is no report on the DOP of the diffracted multi-Gaussian beam. This will be discussed in this manuscript. Firstly, the analytical expressions for the DOP and that for the square of the tangent of the far-field divergence angle of a diffracted multi-Gaussian beam are derived. And then, the influences of the aperture radius, the boundary characteristic, and the beam waist width on the DOP and on the far-field divergence angle are investigated. Additionally, the absolutely decreasing quantity of the DOP induced by the aperture is discussed by contrasting the DOP values for the multi-Gaussian beam with and without the aperture.

2. Theory

As shown in Fig. 1, assume that a multi-Gaussian beam diffracted by an aperture propagates along the z direction from the source plane $z = 0$ into the half-space $z > 0$. The radius of the circular aperture is R , which coincides with the source plane. To analyze the paraxial characteristics of beams, we introduce the definition of DOP, which is given by the formula [17]

$$P = \frac{\iint_{u^2 + v^2 < 1} |A_0(u, v)|^2 \sqrt{1 - (u^2 + v^2)} \, du \, dv}{\iint_{u^2 + v^2 < 1} |A_0(u, v)|^2 \, du \, dv} \quad (1)$$

where $u = p\lambda$, $v = q\lambda$, and $A_0(u, v)$ is the angular spectrum of the beam in the source plane with p and q being the coordinates in spatial-frequency domain, and λ denotes the wavelength in vacuum.

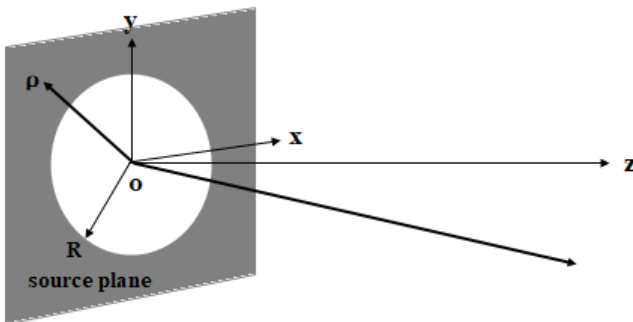


Fig. 1. Illustration of notations.

For a multi-Gaussian beam, its DOP will be influenced as it is diffracted by a circular aperture. To illustrate this effect, let us first recall the field expression of the diffracted multi-Gaussian beam [31-33], *i.e.*,

$$E(\rho, 0) = B \sum_{m=1}^M (-1)^{m-1} C_M^m \exp\left(-m\beta_M \frac{\rho^2}{\sigma^2}\right) \text{circ}(\zeta) \quad (2)$$

where $\rho = (x, y)$ is an arbitrary position vector in the source plane, σ is the beam waist width of a multi-Gaussian beam, B is a constant, M is a non-negative integer which can modulate the boundary characteristic of the source, and $\text{circ}(\zeta)$ is the aperture function which can be expressed as

$$\text{circ}(\zeta) = \begin{cases} 1, & 0 \leq \zeta < 1 \\ 0 & \zeta \geq 1 \end{cases} \quad (3)$$

where $\zeta = \rho/R$. And C_M^m is the binomial coefficient, with a form of

$$C_M^m = \frac{M!}{m!(M-m)!} \quad (4)$$

and

$$\beta_M = -\ln\left[1 - (1 - e^{-1})^{1/M}\right] \quad (5)$$

For a diffracted multi-Gaussian beam, the angular spectrum is given by the Fourier transform of the field function, which can be written as [30]

$$A_0(u, v) = \left(\frac{k}{2\pi}\right)^2 \int_{-\infty}^{+\infty} \int_{-\infty}^{+\infty} E(\rho, 0) \exp[-ik(ux + vy)] dx dy \quad (6)$$

On substituting from Eq. (2) into Eq. (6), the angular spectrum of the diffracted multi-Gaussian beam can be calculated as

$$A_0(u, v) = \frac{\pi\sigma^2 B}{\lambda^2} \sum_{n=1}^{\infty} \frac{2^n \beta^n J_n(\alpha b)}{(\alpha b)^n} \left[\sum_{m=1}^M (-1)^{m-1} C_M^m \exp(-m\beta_M \beta) (m\beta_M)^{n-1} \right] \quad (7)$$

where $b = (u^2 + v^2)^{1/2}$, $\alpha = kR$ and $\beta = R^2/\sigma^2$. $J_n(\alpha b)$ is the first kind Bessel function of order n . In order to obtain above equation, the following formula is used [34]

$$\int x^m J_{m-1}(x) dx = x^m J_m(x) + C \quad (8)$$

The square of the absolute value of the angular spectrum $|A_0(u, v)|^2$ is defined as the angular distribution of energy. After some calculations, $|A_0(u, v)|^2$ is obtained as shown in the following:

$$|A_0(u, v)|^2 = F_1 + F_2 \quad (9)$$

where

$$F_1 = \frac{\pi^2 \sigma^4 B^2}{\lambda^4} \sum_{n=1}^{\infty} \frac{2^{2n} \beta^{2n} J_n^2(\alpha b) H^2(M, n)}{(\alpha b)^{2n}} \quad (10a)$$

$$F_2 = \frac{2\pi^2 \sigma^4 B^2}{\lambda^4} \sum_{n=2}^{\infty} \sum_{l=1}^{n-1} \frac{2^{n+l} \beta^{n+l} J_n(\alpha b) J_l(\alpha b) H(M, n) H(M, l)}{(\alpha b)^{n+l}} \quad (10b)$$

with

$$H(M, n) = \sum_{m=1}^M (-1)^{m-1} C_M^m \exp(-m \beta_M \beta) (m \beta_M)^{n-1} \quad (11a)$$

$$H(M, l) = \sum_{m=1}^M (-1)^{m-1} C_M^m \exp(-m \beta_M \beta) (m \beta_M)^{l-1} \quad (11b)$$

On substituting from Eq. (9) into Eq. (1), and after some calculations, the analytical expression for the DOP of the diffracted multi-Gaussian beam can be expressed as

$$P = \frac{E + F}{G + H} \quad (12)$$

where

$$E = \sum_{n=1}^{\infty} \left(\frac{2\beta}{\alpha} \right)^{2n} H^2(M, n) \int_0^1 J_n^2(\alpha b) \sqrt{1-b^2} b^{-2n+1} db \quad (13a)$$

$$F = 2 \sum_{n=2}^{\infty} \sum_{l=1}^{n-1} \left(\frac{2\beta}{\alpha} \right)^{n+l} H(M, n) H(M, l) \int_0^1 J_n(\alpha b) J_l(\alpha b) \sqrt{1-b^2} b^{-(n+l)+1} db \quad (13b)$$

and

$$G = \sum_{n=1}^{\infty} \left(\frac{2\beta}{\alpha} \right)^{2n} H^2(M, n) \int_0^1 J_n^2(\alpha b) b^{-2n+1} db \quad (14a)$$

$$H = 2 \sum_{n=2}^{\infty} \sum_{l=1}^{n-1} \left(\frac{2\beta}{\alpha} \right)^{n+l} H(M, n) H(M, l) \int_0^1 J_n(\alpha b) J_l(\alpha b) b^{-(n+l)+1} db \quad (14b)$$

To explain the behavior of the DOP, we consider the far-field divergence angle of the diffracted multi-Gaussian beam. The square of the tangent of the far-field divergence angle beyond the validity of the paraxial approximation can be defined as follows [35]

$$\tan^2 \theta = \frac{2 \iint_{u^2+v^2 < 1} \frac{u^2+v^2}{\sqrt{1-(u^2+v^2)}} |A_0(u, v)|^2 du dv}{\iint_{u^2+v^2 < 1} \sqrt{1-(u^2+v^2)} |A_0(u, v)|^2 du dv} \quad (15)$$

On substituting from Eq. (9) into Eq. (15), and after some calculation, the analytical expression for the square of the tangent of the far-field divergence angle can be obtained

$$\tan^2 \theta = \frac{K+L}{E+F} \quad (16)$$

where E and F are given by Eq. (13), and

$$K = 2 \sum_{n=1}^{\infty} \left(\frac{2\beta}{\alpha}\right)^{2n} H^2(M, n) \int_0^1 J_n^2(ab) \frac{b^{-2n+3}}{\sqrt{1-b^2}} db \quad (17a)$$

$$L = 4 \sum_{n=2}^{\infty} \sum_{l=1}^{n-1} \left(\frac{2\beta}{\alpha}\right)^{n+l} H(M, n) H(M, l) \int_0^1 J_n(ab) J_l(ab) \frac{b^{-(n+l)+3}}{\sqrt{1-b^2}} db \quad (17b)$$

In the following, in order to analyze the influence of aperture on the DOP intuitively, we define the absolutely decreasing quantity of the DOP as

$$\Delta P = P_0 - P \quad (18)$$

where P is given by Eq. (12), and P_0 is the DOP of the multi-Gaussian beam without the aperture. If we let the aperture function in Eq. (2) equal to unity, Eq. (2) will reduce to the field of the multi-Gaussian beam without aperture. On substituting this field into Eq. (6), the angular spectrum of the multi-Gaussian beam without aperture can be calculated as

$$A_0(u, v) = \left(\frac{k}{2\pi}\right)^2 B \sum_{m=1}^M (-1)^{m-1} C_M^m \left(\frac{\pi\sigma^2}{m\beta_M}\right) \exp\left[\frac{-k^2\sigma^2}{4m\beta_M}(u^2+v^2)\right] \quad (19)$$

On substituting from Eq. (19) into Eq. (1), after some calculations, we can obtain the analytical expression for P_0 as follows

$$P_0 = \frac{\int_0^1 \left[\sum_{m=1}^M (-1)^{m-1} C_M^m \left(\frac{\pi \sigma^2}{m \beta_M} \right) \exp \left(\frac{-k^2 \sigma^2}{4m \beta_M} t \right) \right]^2 \sqrt{1-t} dt}{\int_0^1 \left[\sum_{m=1}^M (-1)^{m-1} C_M^m \left(\frac{\pi \sigma^2}{m \beta_M} \right) \exp \left(\frac{-k^2 \sigma^2}{4m \beta_M} t \right) \right]^2 dt} \quad (20)$$

Similarly, we can define the absolutely increasing quantity of the square of the tangent of the far-field divergence angle as

$$\Delta T = \tan^2 \theta - \tan^2 \theta_0 \quad (21)$$

where $\tan^2 \theta$ is given by Eq. (16), and $\tan^2 \theta_0$ is the square of the tangent of the far-field divergence angle of the multi-Gaussian beam without aperture. On substituting from Eq. (19) into Eq. (15), the analytical expression for $\tan^2 \theta_0$ can be obtained, with the following form

$$\tan^2 \theta_0 = \frac{2 \int_0^1 \left[\sum_{m=1}^M (-1)^{m-1} C_M^m \left(\frac{\pi \sigma^2}{m \beta_M} \right) \exp \left(\frac{-k^2 \sigma^2}{4m \beta_M} t \right) \right]^2 \frac{t}{\sqrt{1-t}} dt}{\int_0^1 \left[\sum_{m=1}^M (-1)^{m-1} C_M^m \left(\frac{\pi \sigma^2}{m \beta_M} \right) \exp \left(\frac{-k^2 \sigma^2}{4m \beta_M} t \right) \right]^2 \sqrt{1-t} dt} \quad (22)$$

3. Numerical simulations

In this section, in accordance with the analytical expressions of Eq. (12) and Eq. (16), the influences of the aperture and the characteristics of the beam source, such as the

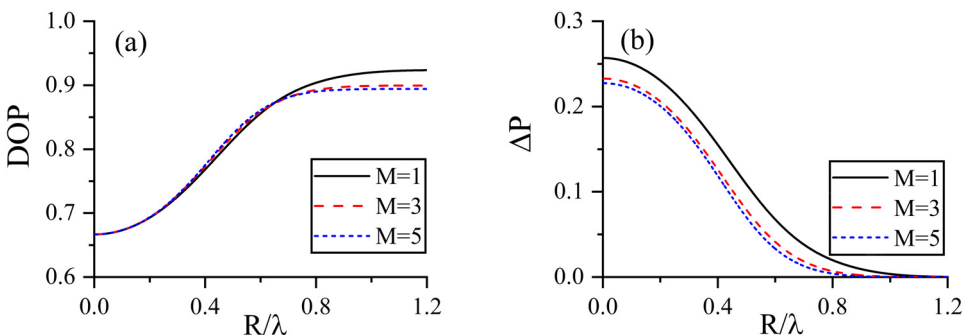


Fig. 2. Dependence of the DOP and the absolutely decreasing quantity ΔP on the ratio R/λ for different boundary characteristic M , respectively. The other parameters are $\lambda = 632.8$ nm, $\sigma = 0.6\lambda$.

aperture radius, the boundary characteristic, and the beam waist width, on the DOP of a diffracted multi-Gaussian beam will be investigated.

Figure 2 presents the dependence of the DOP and the absolutely decreasing quantity ΔP on the ratio R/λ for different boundary characteristic M . In Fig. 2(a), it is shown that when $R/\lambda < 1$, the DOP will increase as R/λ increases, and the dependence of the DOP on the boundary characteristic is not obvious. In the range of $R/\lambda > 1$, the DOP reaches a saturated value, and the larger boundary characteristic is, the smaller saturated value of the DOP will be. In Fig. 2(b), it is shown that with R/λ increasing, ΔP will decrease quickly. When the DOP reaches a saturated value, ΔP tends to be zero. Moreover, ΔP will decrease as the value of M increases, and one can find that the larger boundary characteristic is, the smaller radius under which the DOP reaches a saturated value is.

Figure 3 presents the influence of the beam waist width σ on the DOP and the absolutely decreasing quantity ΔP . It is shown from Figs. 3(a) and (b) that, as the beam waist widths σ are increasing, both the DOP and ΔP will increase. And the beam waist

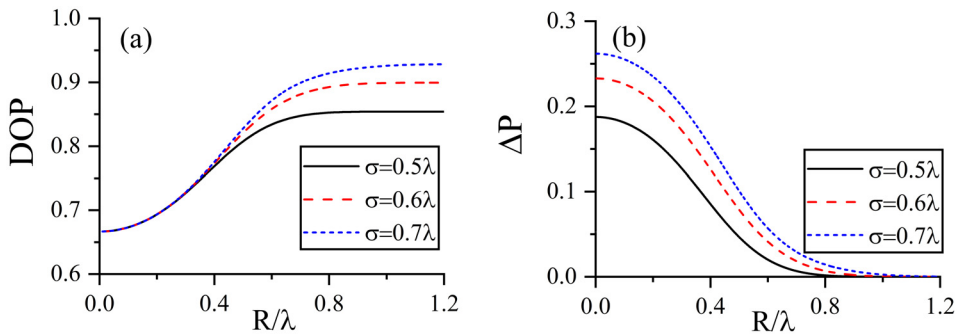


Fig. 3. Dependence of the DOP and the absolutely decreasing quantity ΔP on the ratio R/λ for different beam waist width σ , respectively. The other parameters are $\lambda = 632.8$ nm, $M = 3$.

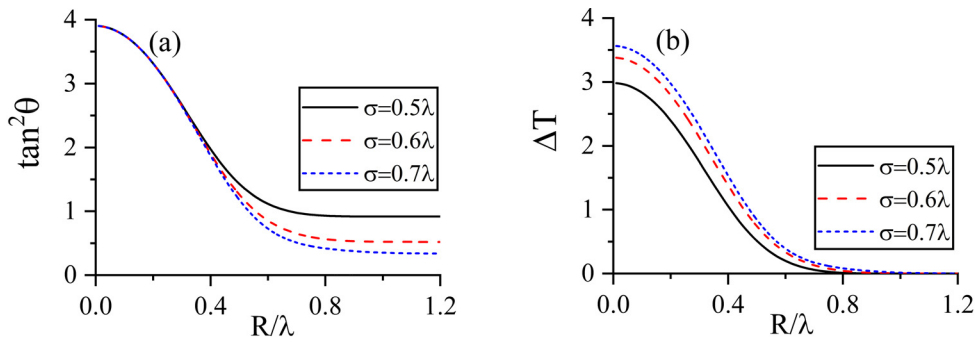


Fig. 4. Dependence of the square of the tangent of the far-field divergence angle $\tan^2\theta$ and the absolutely increasing quantity ΔT on the ratio R/λ for different beam waist width σ , respectively. The other parameters are $\lambda = 632.8$ nm, $M = 3$.

width also plays an important role for the radius under which the DOP and ΔP reach their saturated values.

Figure 4 illustrates the variation of the square of the tangent of the far-filed divergence angle $\tan^2\theta$ and the absolutely increasing quantity ΔT with the ratio R/λ for different beam waist width σ . In Fig. 4(a), when $R/\lambda < 1$, $\tan^2\theta$ shows a trend of sharp decrease as R/λ increases; while in the range of $R/\lambda > 1$, $\tan^2\theta$ tends to be a fixed value, *i.e.*, the influence of the circular aperture on the far-filed divergence angle is negligible. Moreover, it is also shown that the larger beam waist width is, the smaller fixed value will be. In Fig. 4(b), it is shown that ΔT decreases as R/λ increases, until ΔT decreases to zero. In addition, the smaller beam waist width is, the smaller ΔT will be.

Figure 5 shows the dependence of the DOP and the ΔP on the normalized beam waist width σ/λ for different radius R . The DOP and ΔP both increase as the normalized beam waist width σ/λ increases, and when σ/λ becomes large enough, both of them will reach a saturated value. Furthermore, it is demonstrated from Figs. 5(a) and (b) that with the radius R increasing, the DOP will increase while ΔP decrease.

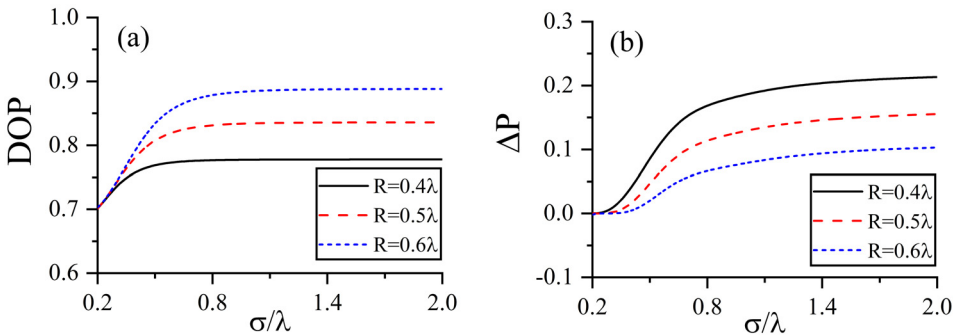


Fig. 5. Dependence of the DOP and the absolutely decreasing quantity ΔP on the normalized beam waist width σ/λ for different radius R , respectively. The other parameters are $\lambda = 632.8$ nm, $M = 3$.

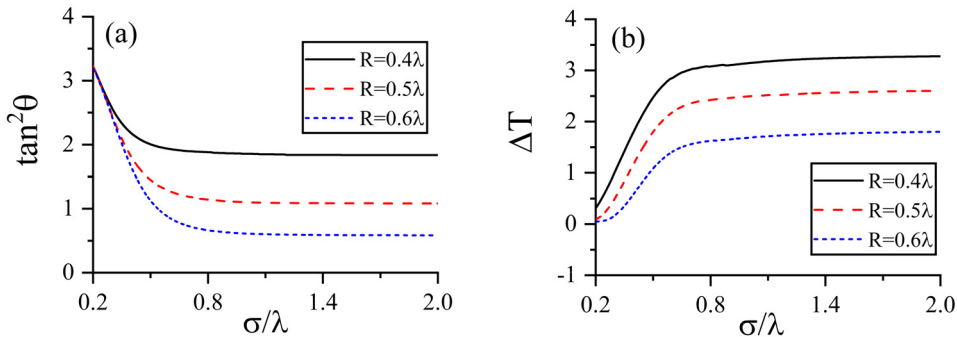


Fig. 6. Dependence of the square of the tangent of the far-filed divergence angle $\tan^2\theta$ and the absolutely increasing quantity ΔT on the normalized beam waist width σ/λ for different radius R , respectively. The other parameters are $\lambda = 632.8$ nm, $M = 3$.

Figure 6 presents the variation of the square of the tangent of the far-field divergence angle $\tan^2\theta$ and the absolutely increasing quantity ΔT on the normalized beam waist width σ/λ for different radius R . As shown in Figs. 6(a) and (b), as σ/λ is gradually increasing, $\tan^2\theta$ and ΔT will reach a saturated value after a sharp decrease and increase, respectively. Additionally, with the radius R increasing, $\tan^2\theta$ and ΔT will demonstrate a similar behavior, *i.e.*, the larger radius R is, the smaller $\tan^2\theta$ and ΔT will be.

4. Conclusions

In conclusion, we have obtained the analytical expression for the DOP of the diffracted multi-Gaussian beam, and discussed the influence of the aperture radius and the characteristics of beam source on the DOP. The result shows that the DOP of the diffracted multi-Gaussian beam is closely related to the boundary characteristics, the beam waist width and the radius of circular aperture. It is also shown that when a multi-Gaussian beam is diffracted by a circular aperture, the DOP will decrease. Moreover, the analytical expression for the square of the tangent of the far-field divergence angle has also been derived, and it is shown that the DOP and the far-field divergence angle show the opposite curve relationship with the change of the same parameters. It should be noted that if the boundary characteristic parameter is chosen to be $M = 1$, the results obtained in this manuscript will reduce to that of Gaussian beam. The results obtained in this manuscript may provide a method to modulate the DOP of the diffracted multi-Gaussian beam, and may have some potential applications in areas such as tight focusing and micro-lithographs.

Acknowledgement

This work was supported by the National Natural Science Foundation of China (NSFC) under grants 11404231, 61775152.

References

- [1] MEI Z., GU J., *Comparative studies of paraxial and nonparaxial vectorial elegant Laguerre-Gaussian beams*, Optics Express **17**, 2009: 14865-14871.
- [2] ZHANG P., HU Y., CANNAN D., SALANDRINO A., LI T., MORANDOTTI R., ZHANG X., CHEN Z., *Generation of linear and nonlinear nonparaxial accelerating beams*, Optics Letters **37**, 2012: 2820-2822.
- [3] DUAN K., LÜ B., *Nonparaxial analysis of far-field properties of Gaussian beams diffracted at a circular aperture*, Optics Express **11**, 2003: 1474-1480.
- [4] HUANG K., WANG X., LIU Z., *Nonparaxial propagation of a rectangular multi-Gaussian Schell-model beam*, Optics Communications **356**, 2015: 25-33.
- [5] LÜ B., DUAN K., *Nonparaxial propagation of vectorial Gaussian beams diffracted at a circular aperture*, Optics Letters **28**, 2003: 2440-2442.
- [6] DUAN K., LÜ B., *Polarization properties of vectorial nonparaxial Gaussian beams in the far field*, Optics Letters **30**, 2005: 308-310.
- [7] GUO L., CHEN L., LIN R., ZHANG M., DONG Y., CHEN Y., CAI Y., *Nonparaxial propagation properties of specially correlated radially polarized beams in free space*, Applied Sciences **9**, 2019: 997-1014.

- [8] DUAN K., LÜ B., *Partially coherent nonparaxial beams*, Optics Letters **29**, 2004: 800-802.
- [9] MOON H., CHOUGH Y., AN K., *Cylindrical microcavity laser based on the evanescent-wave-coupled gain*, Physical Review Letters **85**, 2000: 3161-3164.
- [10] ZHANG Z., PU J., WANG X., *Focusing of partially coherent Bessel–Gaussian beams through a high-numerical aperture objective*, Optics Letters **33**, 2008: 49-51.
- [11] CHEN B., ZHANG Z., PU J., *Tight focusing of partially coherent and circularly polarized vortex beams*, Journal of Optical Society of America A **26**, 2009: 862-869.
- [12] ASHKIN A., *Trapping of atoms by resonance radiation pressure*, Physical Review Letters **40**, 1978: 729-732.
- [13] SUNG S., LEE Y., *Trapping of a micro-bubble by non-paraxial Gaussian beam: Computation using the FDTD method*, Optics Express **16**, 2008: 3463-3473.
- [14] GOMBKÖTÖ B., KOPPA P., SÜTÖ A., LÓRINCZ E., *Computer simulation of reflective volume grating holographic data storage*, Journal of Optical Society of America A **24**, 2007: 2075-2081.
- [15] SUNG Y., SHEPPARD C.J.R., *Three-dimensional imaging by partially coherent light under nonparaxial condition*, Journal of Optical Society of America A **28**, 2011: 554-559.
- [16] EL GAWHARY O., SEVERINI S., *Degree of paraxiality for monochromatic light beams*, Optics Letters **33**, 2008: 1360-1362.
- [17] EL GAWHARY O., SEVERINI S., *Localization and paraxiality of pseudo-nondiffracting fields*, Optics Communications **283**, 2010: 2481-2487.
- [18] DONG Y., ZHANG L., LUO J., WEN W., ZHANG Y., *Degree of paraxiality of coherent and partially coherent Airy beams*, Optics & Laser Technology **49**, 2013: 1-5.
- [19] DONG Y., WANG F., CAI Y., YAO M., *Degree of paraxiality of cylindrical vector partially coherent Laguerre-Gaussian beams*, Optics Communications **333**, 2014: 237-242.
- [20] WANG Z., JIANG Z., JI X., WANG T., *Degree of paraxiality of an electromagnetic multi-Gaussian Schell-model beam*, Journal of Optical Society of America A **36**, 2019: 1033-1038.
- [21] ZHU L., JIANG Z., CHEN K., WANG T., *The degree of paraxiality of an anisotropic generalized multi-Gaussian Schell-model beam*, Journal of Optical Society of America A **35**, 2018: 1034-1038.
- [22] WANG F., CAI Y., KOROTKOVA O., *Degree of paraxiality of a partially coherent field*, Journal of Optical Society of America A **27**, 2010: 1120-1126.
- [23] HUANG J., XIANG S., JIANG W., JI X., WANG T., *Degree of paraxiality of an electromagnetic fractional multi-Gaussian Schell-model beam*, Journal of Optical Society of America A **38**, 2021: 1264-1269.
- [24] EYYUBOĞLU H.T., ARPALI Ç., BAYKAL Y., *Flat topped beams and their characteristics in turbulent media*, Optics Express **14**, 2006: 4196-4207.
- [25] GAO Y., ZHU B., LIU D., LIN Z., *Fractional Fourier transform of flat-topped multi-Gaussian beams*, Journal of Optical Society of America A **27**, 2010: 358-365.
- [26] CHEN J., *Propagation and transformation of flat-topped multi-Gaussian beams in a general nonsymmetrical apertured double-lens system*, Journal of Optical Society of America A **24**, 2007: 84-92.
- [27] GAO Y., ZHU B., LIU D., LIN Z., *Propagation of flat-topped multi-Gaussian beams through a double-lens system with apertures*, Optics Express **17**, 2009: 12753-12766.
- [28] CAI Y., HU L., *Propagation of partially coherent twisted anisotropic Gaussian Schell-model beams through an apertured astigmatic optical system*, Optics Letters **31**, 2006: 685-687.
- [29] ZHOU G., *Far-field structural property of a Gaussian beam diffracted by a phase aperture*, Optics Communications **284**, 2011: 8-14.
- [30] ZHOU G., CHU X., ZHENG J., *Analytical structure of an apertured vector Gaussian beam in the far field*, Optics Communications **281**, 2008: 1929-1934.
- [31] ZHOU G., *Change of the paraxiality of a Gaussian beam diffracted by a circular aperture*, Optics Express **17**, 2008: 8417-8422.
- [32] LI Y., LEE H., WOLF E., *Effect of edge rounding and sloping of sidewalls on the readout signal of the information pits on optical disks*, Optical Engineering **42**, 2003: 2707-2720.
- [33] WANG T., LI X., JI X., ZHAO D., *Spectral changes and spectral switches of light waves on scattering from a semisoft boundary medium*, Optics Communications **324**, 2014: 152-156.

- [34] GRADSHTEYN S., RYZHIK I.M., *Table of Integrals, Series, and Products*, Academic Press, New York, 1980.
- [35] PORRAS M.A., *Non-paraxial vectorial moment theory of light beam propagation*, *Optics Communications* **127**, 1996: 79-95.

*Received January 23, 2023
in revised form April 7, 2023*